A Microscopic Interaction Model of Maximum Solubility of Cholesterol in Lipid Bilayers

Juyang Huang and Gerald W. Feigenson
Section of Biochemistry, Molecular and Cell Biology, Cornell University, Ithaca, New York 14853 USA

ABSTRACT We recently reported the equilibrium maximum solubility of cholesterol in a lipid bilayer, χ^*_{chol}, to be 0.66 in four different phosphatidylcholines, and 0.51 in a phosphatidylethanolamine (Huang, J., J. T. Buboltz, and G. W. Feigenson. 1999. *Biochim. Biophys. Acta.* in press). Here we present a model of cholesterol-phospholipid mixing that explains these observed values of χ^*_{chol}. Monte Carlo simulations show that pairwise-additivity of nearest-neighbor interactions is inadequate to describe all the χ^*_{chol} values. Instead, if cholesterol *multibody* interactions are assigned highly unfavorable energy, then jumps occur in cholesterol chemical potential that lead to its precipitation from the bilayer. Cholesterol precipitation is most likely to occur near three discrete values of cholesterol mole fraction, 0.50, 0.57, and 0.67, which correspond to cholesterol/phospholipid mole ratios of 1/1, 4/3, and 2/1, respectively. At these solubility limits, where cholesterol chemical potential jumps, the cholesterol-phospholipid bilayer mixture forms highly regular lipid distributions in order to minimize cholesterol-cholesterol contacts. This treatment shows that dramatic structural and thermodynamic changes can occur at particular cholesterol mole fractions without any stoichiometric complex formation. The physical origin of the unfavorable cholesterol multibody interaction is explained by an "umbrella model": in a bilayer, nonpolar cholesterol relies on polar phospholipid headgroup coverage to avoid the unfavorable free energy of cholesterol contact with water. Thus, at high cholesterol mole fraction, this unfavorable free energy, *not any favorable cholesterol-phospholipid interaction*, dominates the mixing behavior. This physical origin also explains the "cholesterol condensing effect" and the increase in acyl chain order parameter in cholesterol-phospholipid mixtures.

INTRODUCTION

We seek to understand general properties of biomembranes by exploring the molecular-level interactions among the components. Since there are many chemically different components in a biomembrane, there are very many possibilities for molecular interactions just between nearest-neighbor molecules.

A reasonable starting point toward a description of the molecular-level interactions is to consider a chemically well-defined bilayer mixture of lipids. Cholesterol is the single most abundant molecule in the mammalian plasma membrane, so there have been numerous studies of cholesterol/phospholipid bilayer mixtures (see, for example, Finegold, 1993). In a plasma membrane, cholesterol comprises up to half of all the lipids (Bloch, 1991), and the mole fraction is likely to be even higher in one of the bilayer leaflets.

When the cholesterol content is high enough to exceed the maximum solubility of cholesterol in the lipid bilayer, a mole fraction we refer to as χ^*_{chol}, excess cholesterol molecules leave the bilayer as a precipitate of cholesterol monohydrate crystals. This maximum solubility represents the boundary of a first-order phase transition. Values of χ^*_{chol} that describe this phase boundary in the high-cholesterol regime have been reported in numerous publications, but there is a wide range of disagreement on the actual values (Horowitz et al., 1971; Gershfeld, 1978; Finean, 1990; Bach et al., 1998). Yet, we require a reliable value of χ^*_{chol}, because theoretical studies of cholesterol/phospholipid mixtures offer the best possibility of developing our understanding of the intermolecular interactions only if we can precisely compare the theoretical with the experimental results.

Recently, we discovered that the major source of the disagreement lies in the sample preparation method. Conventional sample preparation methods that pass the mixture through a dry state can induce cholesterol/phospholipid demixing in this dry state (Buboltz and Feigenson, 1999). The cholesterol crystals are carried over to the hydrated lipid dispersions, making the apparent χ^*_{chol} value lower than the true equilibrium value. By using two new independent sample preparation methods that avoid lipid demixing, we were able to find the true equilibrium values of χ^*_{chol} (Huang et al., 1999). These values show a very interesting pattern: for all of the phosphatidylcholines (PCs) studied, regardless of acyl chain type (12:0,12:0 or 16:0,16:0 or 16:0,18:1 or 22:1,22:1) the value of χ^*_{chol} is 0.66 ± 0.01 at 24°C. In contrast, we found the distinctly different result that χ^*_{chol} for (16:0,18:1) phosphatidylethanolamine (PE) is 0.51 ± 0.01. These new findings lead us to ask the following questions: why are the values of χ^*_{chol} insensitive to the type of phospholipid acyl chains? Are some unique properties of cholesterol-phospholipid organization revealed by the observed χ^*_{chol} values, which are very close to cholesterol/phospholipid mole ratios of 1/1 and 2/1? What kind of

Received for publication 2 September 1998 and in final form 19 January 1999.

Address reprint requests to Dr. Gerald W. Feigenson, Section of Biochemistry, Molecular and Cell Biology, Cornell University, 201 Biotechnology Building, Ithaca, NY 14853-2703. Tel.: 607-255-4744; Fax: 607-255-2428; E-mail: GWF3@cornell.edu.

0006-3495/99/04/2142/16 $2.00

microscopic interactions in cholesterol/phospholipid mixtures could give rise to the observed χ^*_{chol} values of 0.66 and 0.51?

In this study we present a microscopic interaction model that answers these questions. We used Monte Carlo simulation as a tool to translate our model into the corresponding chemical potentials and lipid lateral organizations. We find that pairwise-additive interactions *can* explain a value of $\chi^*_{chol} = 0.51$, if mixing of phospholipid with cholesterol is sufficiently strongly favorable. However, this simple model *cannot* predict $\chi^*_{chol} = 0.66$. We find that if a simple form of multibody interaction is used, in which cholesterol-cholesterol interaction energy becomes unfavorable more steeply than additively for more cholesterols in contact, then χ^*_{chol} of either 0.51 or 0.66 can occur, depending upon the details of the nonlinear energy increase. Moreover, a value of $\chi^*_{chol} = 0.57$ is also shown to be possible. Our simulations show that at the solubility limits, highly regular lipid distributions form in the bilayer, and the chemical potential of cholesterol jumps steeply. The physical origin of this multibody interaction can be explained by the hydrophobicity of cholesterol.

BASIC ASSUMPTIONS AND STRATEGY

Chemical potential of cholesterol

Cholesterol in a monohydrate crystal, as a pure substance, has a constant chemical potential, $\mu^{crystal}_{chol}$. In contrast, the chemical potential of cholesterol in a lipid bilayer, $\mu^{bilayer}_{chol}$ (χ_{chol}), is a function of the bilayer composition. When $\chi_{chol} < \chi^*_{chol}$, $\mu^{bilayer}_{chol}$ (χ_{chol}) must be *less* than $\mu^{crystal}_{chol}$ for the bilayer to be the only stable phase. When $\chi_{chol} \geq \chi^*_{chol}$, the lipid bilayer phase and the cholesterol monohydrate crystal phase coexist. In this two-phase region, the chemical potential of cholesterol in the bilayer must be equal to the chemical potential of cholesterol in the monohydrate crystal, $\mu^{bilayer}_{chol}$ (χ^*_{chol}) = $\mu^{crystal}_{chol}$.

A key experimental finding is the essentially identical values of χ^*_{chol} in four PCs having different sets of acyl chains. This finding leads us to deduce a general picture of the way in which cholesterol chemical potential changes as its mole fraction increases in a bilayer. The theoretical treatment will be designed to search for the microscopic energies that reproduce this form of the chemical potential change.

We start with the chemical potential of cholesterol, at any given mole fraction, being different in phospholipids A, B, and C. A very simple form of this difference would be a constant offset of the cholesterol chemical potential at every mole fraction in the three phospholipid environments. Fig. 1 illustrates a general relationship between the shape of the $\mu^{bilayer}_{chol}$ profile and the range of possible χ^*_{chol} values. This figure also shows the chemical potential of cholesterol in the pure monohydrate crystal, $\mu^{crystal}_{chol}$, as a horizontal dashed line. In Fig. 1 *a*, a hypothetical $\mu^{bilayer}_{chol}$ curve in phospholipid A is drawn as a smoothly increasing function of χ_{chol}

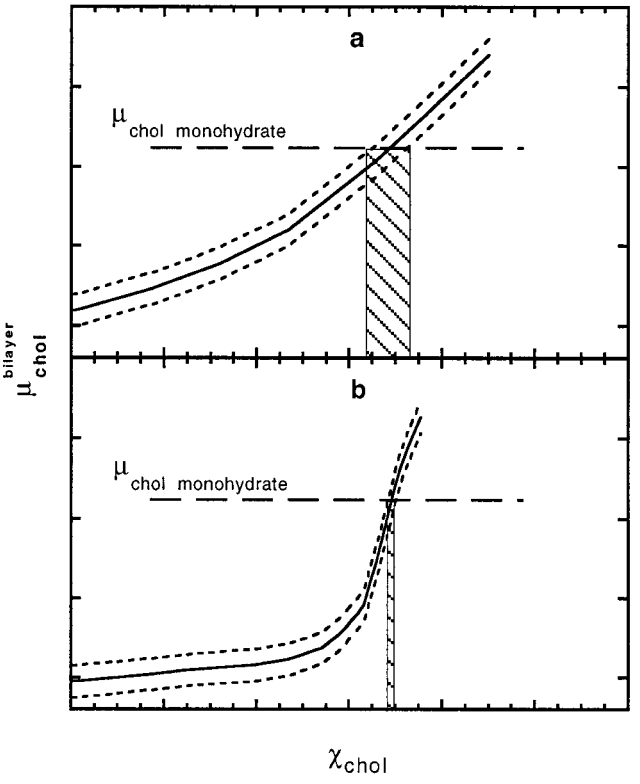

FIGURE 1 Relationship between the shape of $\mu^{bilayer}_{chol}$ profiles and the range of possible χ^*_{chol} values. (*a*) A set of hypothetical $\mu^{bilayer}_{chol}$ profiles as smoothly increasing functions of χ_{chol}. The range of the χ^*_{chol} values is indicated by the width of the shaded box. (*b*) A set of hypothetical $\mu^{bilayer}_{chol}$ profiles as steeply increasing functions of χ_{chol}. The range of the χ^*_{chol} values is much narrower.

(*solid line*). The cholesterol mole fraction at which $\mu^{bilayer}_{chol}$ intersects the chemical potential of crystalline cholesterol monohydrate is the χ^*_{chol} value in lipid A. Consider two other phospholipids, B and C, with different sets of acyl chains, and having cholesterol-phospholipid interactions that are slightly different from those in lipid A. The $\mu^{bilayer}_{chol}$ profiles in phospholipids B and C would be slightly different from that in phospholipid A. We represent these profiles as the two dotted lines in Fig. 1 *a*, obtained by adding or subtracting a small constant offset to or from the $\mu^{bilayer}_{chol}$ of lipid A. These two dotted lines intersect $\mu^{crystal}_{chol}$ at different values of χ_{chol}, thus resulting in different values of χ^*_{chol}. The range of χ^*_{chol} values for lipids A, B, and C is indicated by the width of the shaded box. In Fig. 1 *b*, a hypothetical $\mu^{bilayer}_{chol}$ curve is drawn having a steep increase at some cholesterol mole fraction. With the same offset of chemical potential at each cholesterol mole fraction, the resulting range of χ^*_{chol} is much narrower. Since the χ^*_{chol} for four PCs with very different acyl chains are almost identical, *whatever is the nature of the microscopic interaction that induces the cholesterol precipitation, it must cause the chemical potential of cholesterol in the bilayer to increase so sharply at* χ^*_{chol} *that other contributions can be neglected.*

Single-state lattice model

The above analysis implies that we can safely ignore the variation of $\mu_{chol}^{bilayer}$ in each different acyl chain environment, since it does not show up in the measured value of χ_{chol}^{*}, as long as it is not of comparable energy. That is, the acyl chain contribution to the chemical potential does *not* need to be assumed as zero, yet *we can completely ignore acyl chain details in our model, and instead need only note whether or not there is an acyl chain or a cholesterol at a given lattice position.*

The general mixing behavior of cholesterols near χ_{chol}^{*}

Since $\mu_{chol}^{bilayer}$ (χ_{chol}) is a steeply increasing function of χ_{chol} near χ_{chol}^{*}, the *excess* chemical potential of cholesterol should be a steeply increasing function as well, because the ideal part of the chemical potential (RTln χ_{chol}) is a slowly increasing function around $\chi_{chol} = 0.5$ or 0.67. Thus, the microscopic interaction that induces cholesterol precipitation strongly favors the mixing of cholesterol with phospholipid. Otherwise, if cholesterol molecules tended to cluster, the excess chemical potential of cholesterol would decrease as a function of χ_{chol}, instead of increase. In terms of microscopic interaction energy, *cholesterol-cholesterol contacts are unfavorable or cholesterol-phospholipid contacts are favorable.*

Type of lattice

The cross-sectional area of cholesterol is ~37 Å^2 (Lundberg, 1982), that of a fluid phase phospholipid is on the order of 65 Å^2 (Nagle et al., 1996). Other researchers have modeled the packing of cholesterol molecules and phospholipid acyl chains as a hexagonal lattice (Cruzeiro-Hansson et al., 1989; Scott, 1991). The justification for using a lattice of *acyl chains* and cholesterol, rather than *entire phospholipids* and cholesterol, has been discussed by Virtanen et al. (1995). We, too, will use the hexagonal packing model of acyl chains and cholesterol in this study. Since the sizes and packing details are surely not identical for cholesterol and phospholipid acyl chains, a distorted hexagonal lattice seems likely. Such a distorted hexagonal lattice will serve our purpose well, as long as each site has six nearest-neighbors. As we discussed above with reference to Fig. 1, we assume that all possible variations of the acyl chains (length, conformation, unsaturation) yield only one energy state, and all the interactions with neighbors as well as any conformation changes on any parts of either the phospholipid or the cholesterol are included in the phenomenological interaction energy terms. In addition, although phospholipid headgroups and water molecules are not shown explicitly in the lattice, their effects are implicit in the phenomenological acyl chain-cholesterol interaction.

Our goal is to formulate a simple and general form of the microscopic cholesterol/phospholipid interaction Hamiltonian that could cause an abrupt increase of cholesterol chemical potential at $\chi_{chol} = 0.66$ or 0.51. We use Monte Carlo simulations as the tool to find the microscopic interactions: a hypothetical interaction Hamiltonian is fed into the simulations; the simulations faithfully produce the corresponding free energy, chemical potentials, and molecular distributions of the simulated mixtures; the simulation results are then compared to the experimental data, and the Hamiltonian modified for a better fit.

THE MICROSCOPIC INTERACTION MODEL

The cholesterol/phospholipid bilayer is modeled as a two-dimensional hexagonal lattice. Each lattice site can be occupied by either a phospholipid acyl chain or a cholesterol molecule. We model the interactions between phospholipids and cholesterols in the simplest possible way by limiting all the interactions to nearest-neighbor only. The Hamiltonian has two major components: one describing pairwise-additive interactions, H_{pair}, and another for cholesterol multibody interactions with its nearest-neighbors, H_{multi}.

$$H_{total} = H_{pair} + H_{multi} \tag{1}$$

The pairwise-additive part of the Hamiltonian includes the interactions of acyl chain-acyl chain, cholesterol-cholesterol, and acyl chain-cholesterol contact pairs:

$$H_{pair} = \frac{1}{2}\sum_{i,j} E_{aa}L_{ai}L_{aj} + \frac{1}{2}\sum_{i,j} E_{cc}L_{ci}L_{cj} + \frac{1}{2}\sum_{i,j} E_{ac}(L_{ai}L_{cj} + L_{ci}L_{aj}) \tag{2}$$

where E_{aa}, E_{cc}, and E_{ac} are the interaction energies between acyl chains, between cholesterols, and between acyl chain-cholesterol, respectively; L_{ai} and L_{ci} are the occupation variables (= 0 or 1) of acyl chains and cholesterols, respectively. The summation i is over all lattice sites, and j is over the nearest-neighbor sites of i only. The factor 1/2 is necessary to avoid counting each contact pair twice.

For this lattice system, the three interaction energies in Eq. 2 can be further reduced to just one independent variable (Guggenheim, 1952). Eq. 2 is rewritten as:

$$H_{pair} = \frac{Z}{2}\sum_{i} E_{aa}L_{ai} + \frac{Z}{2}\sum_{i} E_{cc}L_{ci} + \frac{1}{2}\sum_{i,j} \Delta E_m(L_{ai}L_{cj} + L_{ci}L_{aj}), \tag{3}$$

where Z is the number of nearest-neighbors to a lattice site, which is six for a hexagonal lattice. ΔE_m is the pairwise-additive excess mixing energy of acyl chains and cholesterols, defined as

$$\Delta E_m = E_{ac} - (E_{aa} + E_{cc})/2. \tag{4}$$

In a canonical Monte Carlo simulation, the total number of lattice sites (N), the number of acyl chains ($N_a = \Sigma_i L_{ai}$), the number of cholesterols ($N_c = \Sigma_i L_{ci}$), and the temperature (T) are all fixed for each simulation. Therefore, the first two terms in Eq. 3 are independent of lipid lateral distribution, and the entire contribution of pairwise-additive interactions to the lipid mixing behavior is determined by the value of ΔE_m in the third term.

The cholesterol multibody interaction with its six nearest-neighbors is given by:

$$H_{\text{multi}} = \sum_i \sum_{s=0}^{6} \Delta E_c C_s L_{si} L_{ci}, \tag{5}$$

where ΔE_c is the strength of the cholesterol multibody interaction, C_s are the energy scaling factors, and L_{si} is the environment variable of a lattice site, which is defined as

$$L_{si} = \begin{cases} 1, & \text{if site } i \text{ has } s \text{ cholesterol as it nearest neighbor} \\ 0, & \text{otherwise.} \end{cases}$$

In Eq. 5, the summation s is over seven possible environments for lattice site i: a site can have zero to six cholesterols as nearest-neighbors. Thus, if a cholesterol is surrounded by s other cholesterols, then the multibody interaction energy for this cholesterol would be $\Delta E_c C_s$. No energy difference is assumed for the different arrangements of these s cholesterols among the nearest-neighbor sites. Seven energy scaling factors ($C_0, C_1, \ldots, C_6$) define the relative magnitude of the multibody interaction in the seven possible situations, and ΔE_c determines the overall strength of the cholesterol multibody interaction. The physical origin of this multibody interaction term is described in the Discussion.

SIMULATION METHOD

All the simulations were performed on a 120 × 120 hexagonal lattice with a standard periodical boundary condition. Neighboring cholesterols and acyl chains can exchange their position with a probability given by the Metropolis method (Metropolis et al., 1953). All simulations started from an ideal mixture of given composition. Equilibrium conditions were established after an initial 25,000–70,000 Monte Carlo steps. The ensemble average of the data was obtained in 10,000 Monte Carlo steps after equilibrium. Data were averaged from three independent runs. As demonstrated in an earlier paper (Huang and Feigenson, 1993), such a large-scale simulation makes the simulation size effect negligible.

FREE ENERGY AND CHEMICAL POTENTIALS

In order to relate our microscopic interaction model to experimental χ^*_{chol} data, it is crucial to be able to calculate the chemical potential of cholesterol from computer simulations. We applied the Kirkwood coupling parameter method (Haile, 1986; Chialvo, 1990; Kirkwood, 1935, 1936) to calculate the excess Gibbs free energy of the cholesterol/phospholipid mixtures. Although this approach is computationally intensive, it provides complete information: mixing free energy, enthalpy, entropy, and chemical potentials of cholesterol and acyl chains.

Following similar steps described in our earlier paper (see Appendix in Huang et al., 1993), the excess Gibbs free energy of a cholesterol/phospholipid mixture is given by

$$\Delta G^E(\Delta E_m, \Delta E_c) = N_0 \int_0^{\Delta E_m} \frac{\left\langle \frac{1}{2} \sum_{i,j} (L_{ai} L_{cj} + L_{ci} L_{aj}) \right\rangle_{\lambda_c = 0}}{N} d\lambda_E + N_0 \int_0^{\Delta E_c} \frac{\left\langle \sum_i \sum_{s=0}^{6} C_s L_{si} L_{ci} \right\rangle_{\lambda_E = \Delta E_m}}{N} d\lambda_C - N_0 \Delta E_c C_6 \frac{N_c}{N} \tag{6}$$

where N_0 is Avogadro's number, λ_E and λ_C are coupling parameters, and the angle brackets denote an ensemble average from Monte Carlo simulations. By performing numerical integration, ΔG^E can be calculated. The excess enthalpy ΔH^E and entropy ΔS^E are given by:

$$\Delta H^E = N_0 \left\langle \frac{1}{2} \sum_{i,j} (L_{ai} L_{cj} + L_{ci} L_{aj}) \right\rangle \Delta E_m / N + N_0 \left\langle \sum_i \sum_{s=0}^{6} C_s L_{si} L_{ci} \right\rangle \Delta E_c / N - N_0 \Delta E_c C_6 N_c / N \tag{7}$$

and

$$\Delta S^E = (\Delta H^E - \Delta G^E)/T \tag{8}$$

The excess chemical potentials of cholesterol and phospholipid (μ^E_{chol} and μ^E_{lipid}) can be obtained by differentiating ΔG^E,

$$\Delta G^E = \mu^E_{\text{chol}} N_c / N + \mu^E_{\text{lipid}} N_a / N \tag{9}$$

For convenience, we choose the standard state of μ^E_{chol} as that in which cholesterols are infinitely dilute in a phospholipid bilayer, and the standard state of μ^E_{lipid} as that in a pure phospholipid bilayer.

Since each phospholipid has two acyl chains (see Note 1 at end of text) the mole fraction of cholesterol in a bilayer is given by

$$\chi_{\text{chol}} = 2N_c/(2N_c + N_a). \tag{10}$$

COMPUTER SIMULATION RESULTS

Pairwise-additive interaction energies

First, we investigate the effects of a pairwise-additive interaction energy on the chemical potential and the molecular distributions. As shown above, three interaction energies (E_{aa}, E_{cc}, and E_{ac}) can be specified for a mixture, but these can be reduced to a single parameter ΔE_m (Eq. 4), which dictates the mixing behavior: 1) $\Delta E_m = 0$, ideal mixing. Excess Gibbs free energy = 0; 2) $\Delta E_m > 0$, mixtures tend to form clusters of like molecules, and even lateral phase separation is possible (Huang and Feigenson, 1993); 3) $\Delta E_m < 0$, cholesterol and acyl chains are mixed better than randomly. Like molecules tend to separate from each other. The excess chemical potential of cholesterol increases with increase of χ_{chol}, which is consistent with the general mixing behavior of cholesterol deduced from the χ^*_{chol} data. This is the case we shall study.

Fig. 2 *a* shows excess Gibbs free energies versus χ_{chol} for some negative values of ΔE_m. These negative values of ΔG^E indicate that the Gibbs free energies are lowered by mixing phospholipids with cholesterols. Fig. 2 *a* has a distinct feature that ΔG^E has a sudden change in slope at about $\chi_{chol} = 0.5$ when $\Delta E_m \leq -2$ kT, indicating a new regime of lateral organization of the molecules.

Fig. 3 shows some snapshots of acyl chain/cholesterol lateral distributions simulated using pairwise-additive interactions. Each filled circle represents one cholesterol molecule, each open circle a phospholipid acyl chain. As shown in Fig. 3 *a,* at $\chi_{chol} = 0.5$, with a low magnitude of ΔE_m (-1 kT), the distribution has no particular pattern: some cholesterol molecules have no cholesterol-cholesterol contact, others have up to four contacts. However, at the same composition, with $\Delta E_m = -3$ kT, cholesterol molecules form a crystal-like regular pattern (Fig. 3 *b*): each cholesterol is surrounded by six acyl chains, and cholesterol-cholesterol contacts are minimized. Although some minor defects are common, the order is very long-range, only limited by the simulation size. Fig. 3, *c* and *d* are snapshots of the lateral distributions simulated with $\Delta E_m = -3$ kT at $\chi_{chol} = 0.44$ and 0.56, respectively, slightly below or above $\chi_{chol} = 0.5$. As χ_{chol} increases, the crystal-like regular pattern gradually grows in size at lower concentration, encompasses the whole lattice at the critical composition, then is gradually destroyed when χ_{chol} becomes higher.

The effect of this crystal-like regular distribution on chemical potential of cholesterol is shown in Fig. 4 *a.* When the value of ΔE_m is small, $\mu^{bilayer}_{chol}$ increases smoothly as a function of χ_{chol}. With a large negative value of ΔE_m, $\mu^{bilayer}_{chol}$ shows a jump at $\chi_{chol} = 0.5$. The magnitude of the jump increases with the magnitude of ΔE_m.

The formation of the crystal-like regular distribution pattern and the sharp increase of $\mu^{bilayer}_{chol}$ at $\chi_{chol} = 0.5$ can be easily understood. A large negative value of ΔE_m makes like-molecule contact very unfavorable (or equivalently, unlike-molecule contact very favorable). Energy is lowered

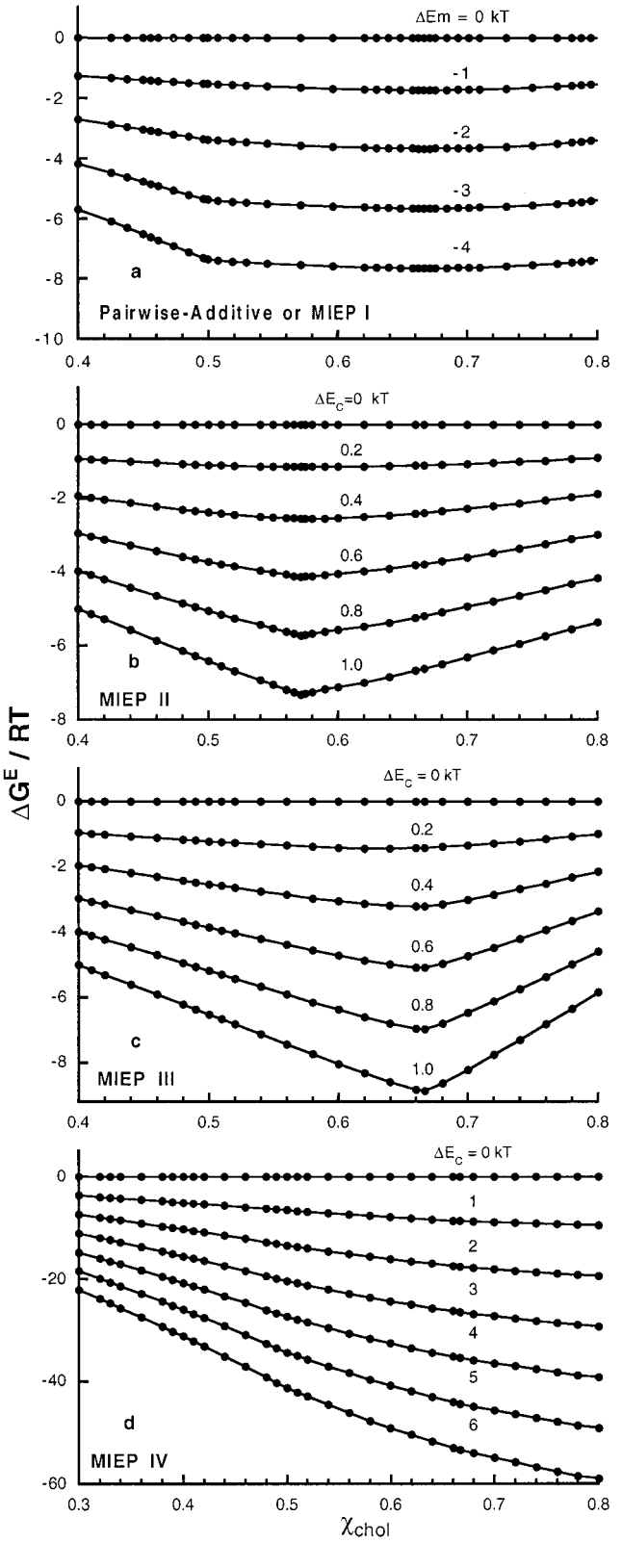

FIGURE 2 Excess Gibbs free energy, ΔG^E, as a function of cholesterol mole fraction in a bilayer. Simulations use: (*a*) pairwise-additive interactions, which is equivalent to MIEP I; (*b*) MIEP II; (*c*) MIEP III; (*d*) MIEP IV.

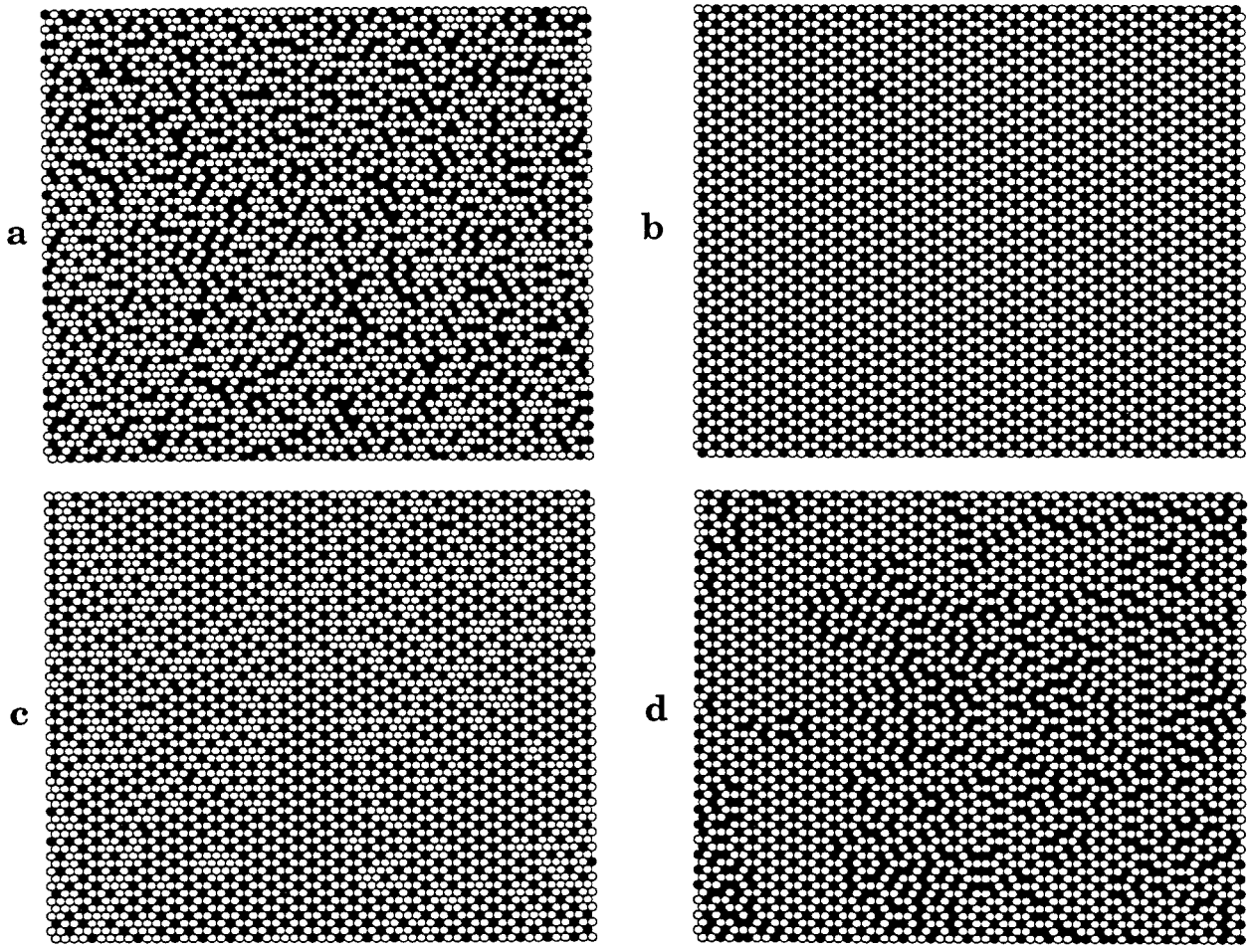

FIGURE 3 Snapshots of phospholipid and cholesterol lateral distributions simulated using pairwise-additive interactions. (*a*) $\chi_{chol} = 0.50$ and $\Delta E_m = -1$ kT; (*b*) $\chi_{chol} = 0.50$ and $\Delta E_m = -3$ kT. Cholesterols form a crystal-like regular distribution pattern: each cholesterol has no other cholesterol as its nearest neighbor; (*c*) $\chi_{chol} = 0.44$ and $\Delta E_m = -3$ kT; (*d*) $\chi_{chol} = 0.56$ and $\Delta E_m = -3$ kT. (●) Cholesterol; (○) acyl chain.

by minimizing cholesterol-cholesterol contacts or maximizing acyl chain-cholesterol contacts. At $\chi_{chol} = 0.5$, the ratio of acyl chain to cholesterol is exactly 2/1. The crystal-like regular pattern shown in Fig. 3 *b* is the *only* distribution that avoids any cholesterol-cholesterol contact at this composition. The chemical potential of cholesterol in such a perfect pattern is still low. Now imagine that a tiny amount of cholesterol is added to the mixture, replacing phospholipid, to raise χ_{chol} by an infinitesimal amount just above 0.5: each added cholesterol now occupies a site previously occupied by an acyl chain, and would have *three* cholesterol-cholesterol contacts in such a pattern (see Fig. 3 *b*). The energy cost for such an operation (losing three acyl chain-cholesterol contacts) is very high, with a large negative value of ΔE_m. Therefore, the chemical potential of cholesterol just above $\chi_{chol} = 0.5$ rises sharply.

In order to induce a sharp jump in chemical potential of cholesterol, ΔE_m must be ≤ -2 kT (Fig. 4 *a;* see Note 2). This ΔE_m could arise from a -2 kT favorable interaction energy between an acyl chain-cholesterol pair or from a $+4$ kT unfavorable interaction energy between a cholesterol-cholesterol pair, or from some combination (Eq. 4).

Need for the multibody interaction

Fig. 4 *a* shows that besides $\chi_{chol} = 0.5$, the chemical potential of cholesterol has *no sharp increase at any other composition* (see Note 3). Therefore, no matter how the three interaction energies (E_{aa}, E_{cc}, and E_{ac}) are chosen to formulate ΔE_m (using Eq. 4), it is impossible to produce a sharp increase of $\mu_{chol}^{bilayer}$ at $\chi_{chol} = 0.67$ by a pairwise-additive interaction Hamiltonian. This suggests that a new form of the interaction is needed. As we show in the next section, a relatively simple form of the cholesterol multibody interaction can produce a sharp increase of $\mu_{chol}^{bilayer}$ either at $\chi_{chol} = 0.5$, or 0.57, or 0.67. The pairwise-additive term we studied in this section can be seen as a special case of the multibody interaction.

The cholesterol multibody interaction energy

In the previous section we saw the limitation of the pairwise-additive interaction Hamiltonian. The main question still remains: how to formulate a simple and general microscopic cholesterol/phospholipid interaction Hamiltonian

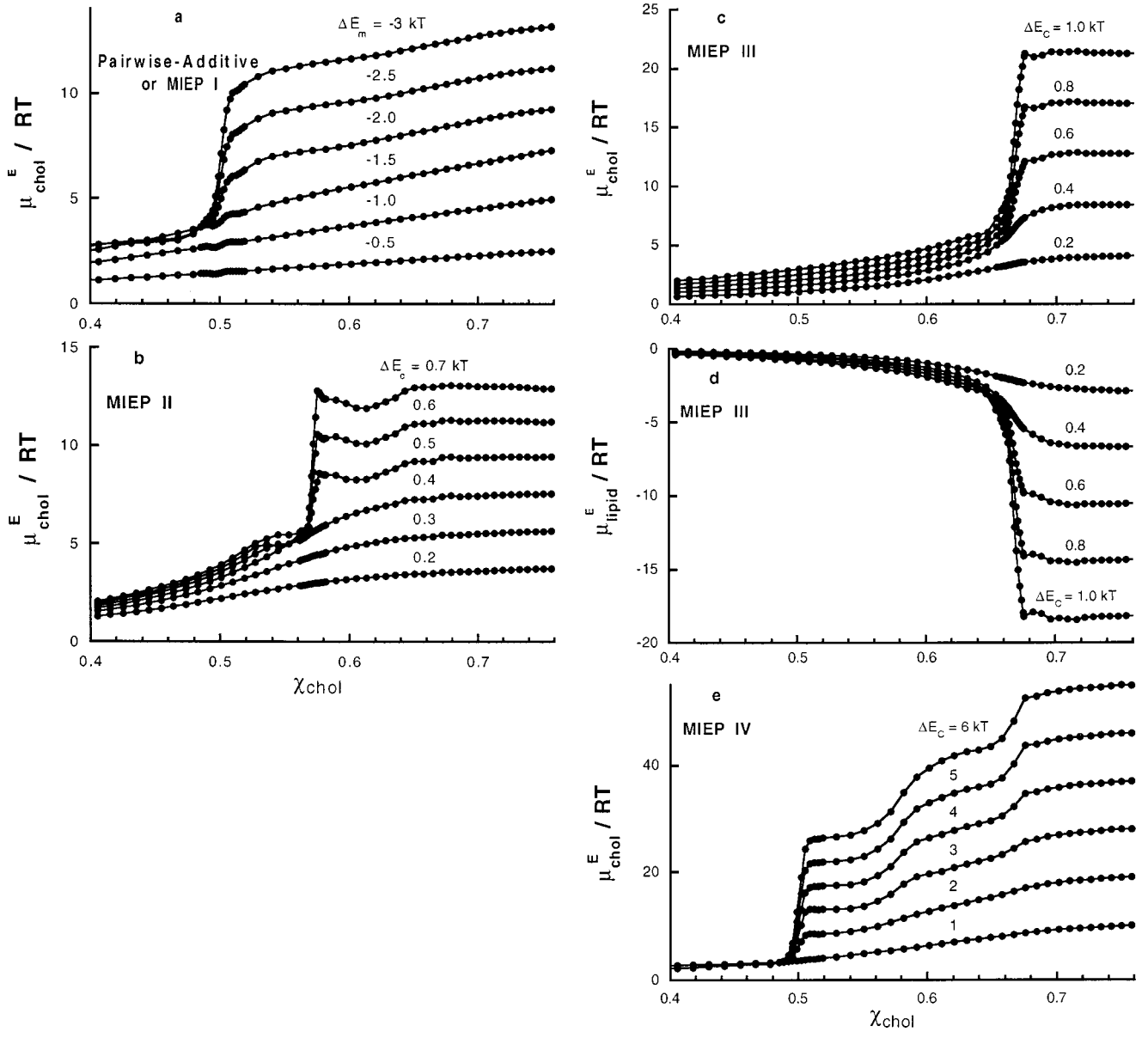

FIGURE 4 Excess chemical potential of cholesterol, μ^{E}_{chol}, or of phospholipid, μ^{E}_{lipid}, as a function of cholesterol mole fraction. (*a*) μ^{E}_{chol} simulated using pairwise-additive interactions, which is equivalent to MIEP I; (*b*) μ^{E}_{chol}, simulated using MIEP II; (*c*) μ^{E}_{chol} and (*d*) μ^{E}_{lipid}, simulated using MIEP III; (*e*) μ^{E}_{chol}, simulated using MIEP IV.

that could cause an abrupt increase of cholesterol chemical potential at $\chi_{chol} = 0.67$ or 0.50. Since no pairwise-additive term will work, using a multibody interaction is a natural solution. However, unlike the pairwise-additive interaction shown in Eq. 2, there is no general form for the multibody interaction. Although there are many possibilities for the type of multibody interactions (e.g. 3 body, 4 body, . . .), in a hexagonal lattice, a reasonable choice would be one involving all six nearest-neighbors. After a period of extensive simulation work, we discovered that a simple and reasonable form for the multibody interaction given in Eq. 5 can solve the problem.

We start by noting that for a pairwise-additive interaction the number of such pairs is counted, and the total interaction energy increases *linearly* with the number of interaction pairs. For example, in Eq. 2 E_{cc} is the interaction energy for a cholesterol-cholesterol pair. If there are n cholesterol-cholesterol contacts, then the total energy is simply nE_{cc}. Thus, the total pairwise-additive energy is the *sum* of the energies of each individual pair.

In contrast, the multibody interaction energy is a description of the interactions of all nearest neighbors considered as a group. The multibody interaction Hamiltonian in Eq. 5 allows the total interaction energy to increase *nonlinearly* with the number of cholesterol-cholesterol contacts. For example, if a cholesterol has two cholesterol-cholesterol contacts, the interaction energy would be $c_2\Delta E_c$ instead of $2\Delta E_c$. Here c_2 is a chosen constant. Thus, six parameters,

$c_1 \ldots c_6$ (c_0 is always 0) need to be specified for the multibody interaction in a hexagonal lattice.

Table 1 lists four sets of multibody interaction energy parameters (MIEP) used in this study. For example, in MIEP II, the energy cost of the first cholesterol-cholesterol contact is 1 unit, for the second one 8 units, the third 3 units, and so on. Thus, $c_1 = 1$, $c_2 = 1 + 8 = 9$, $c_3 = 1 + 8 + 3 = 12$, and so on. These sets describe, although not uniquely, how the energy increases as cholesterols make contact with each other, for positive values of ΔE_c.

The first set, MIEP I, is constructed to create a significant but equal energy cost for each cholesterol-cholesterol contact. Therefore, the total energy increases *linearly* with the number of cholesterol-cholesterol contacts (indicated by the linear increase of $c_1, \ldots, c_6$). With MIEP I, the multibody interaction Hamiltonian is reduced to a pairwise-additive Hamiltonian with $E_{aa} = E_{ac} = 0$, $E_{cc} = 2\Delta E_c$, and $\Delta E_m = -\Delta E_c$ (using Eq. 4). Therefore, we can consider that the results from the previous section were obtained using MIEP I.

The second set, MIEP II, is constructed to create a relatively small energy cost for each pair of cholesterols that are in contact but completely surrounded by phospholipids, with a much larger energy cost for three cholesterols in contact. The first cholesterol-cholesterol contact costs 1 unit of energy, whereas the next one costs 8 energy units, thus much higher than the first. Contacts that are even higher-order are not so critical, so all are assigned to 3 units. Fig. 2 *b* shows the excess Gibbs free energy versus χ_{chol} simulated using MIEP II. The values of ΔG^E are negative, indicating that the Gibbs free energies are lowered by mixing phospholipids with cholesterols. ΔG^E has a global minimum as well as a sudden change of slope at $\chi_{chol} = 0.57$ (cholesterol/phospholipid mole ratio of 4/3). Fig. 4 *b* shows the excess chemical potential of cholesterol versus χ_{chol}; μ^E_{chol} has a sharp jump at 0.57 for $\Delta E_c \geq 0.5$ kT.

Fig. 5 shows snapshots of cholesterol and acyl chain lateral distributions simulated with MIEP II. With a low magnitude of ΔE_c (0.2 kT), as shown in Fig. 5 *a,* at $\chi_{chol} = 0.57$ the distribution shows no particular pattern. However, at the same composition, with $\Delta E_c = 0.5$ kT, cholesterol molecules form an aligned dimer pattern (Fig. 5 *b*): each cholesterol has exactly one cholesterol-cholesterol contact. Figs. 5 *c* and 7 *d* are snapshots of the lateral distributions simulated with $\Delta E_c = 0.5$ kT at $\chi_{chol} = 0.51$ and 0.62, respectively. At $\chi_{chol} = 0.51$, many cholesterol dimers have formed, but no one preferred orientation is adopted (Fig. 5 *c*); at the critical mole fraction of 0.57, all dimers are perfectly aligned to one orientation (Fig. 5 *b*); at $\chi_{chol} = 0.62$, the dimer pattern no longer exists (Fig. 5 *d*).

By understanding this dimer pattern, one can understand how other multibody interaction sets work. The formation of the dimer pattern and abrupt increase of $\mu^{bilayer}_{chol}$ at $\chi_{chol} = 0.57$ are direct results of this particular choice of the multibody interaction parameters. In Table 1, MIEP II is deliberately formulated to make the second contact cost much more energy than the first. The energy cost for other, higher-order contacts are not critical to produce the dimer pattern, as long as they are positive, so we chose 3 for them. The mixture responds to MIEP II with a distribution that minimizes the second cholesterol-cholesterol contact, as shown in Fig. 5 *b.* At $\chi_{chol} = 0.57$, the cholesterol/acyl chain ratio is 2/3. The dimer pattern is the only pattern at this composition such that no cholesterol has the second cholesterol-cholesterol contact, i.e., the lowest energy distribution.

Consider a tiny amount of cholesterol added to the mixture, replacing acyl chains and raising χ_{chol} by an infinitesimal amount above 0.57. The added cholesterol would be forced into sites previously occupied by acyl chains with either three or four cholesterol contacts (Fig. 5 *b*). This newly added cholesterol now touches the three or four nearest-neighbor cholesterols that already have a second cholesterol-cholesterol contact. The energy cost for such an operation would be very high. Therefore, the chemical potential of cholesterol sharply jumps at $\chi_{chol} = 0.57$.

In MIEP II, the second cholesterol-cholesterol contact is assigned to cost 8 energy units. In order to induce a sharp jump in chemical potential of cholesterol, ΔE_c should be $\geq$0.5 kT (Fig. 4 *b*). Thus, the actual energy cost for the second cholesterol-cholesterol contact should be $0.5 \times 8 = 4$ kT or higher.

Fig. 5 *e* shows a metastable distribution at $\chi_{chol} = 0.57$ simulated with $\Delta E_c = 0.6$ kT. There are multiple domains of aligned dimer patterns in this distribution, and each domain has its own orientation. In a hexagonal lattice, three such orientations are possible. At the domain boundaries, many cholesterol trimers are visible, which indicates that the energy of this multidomain distribution is higher than that of the single-domain distribution shown in Fig. 5 *b*. We found that this metastable distribution at high ΔE_c is very persistent in simulations: it could not be relaxed to a single-domain distribution even with very long simulation times (up to 1,000,000 steps). However, it is possible to avoid the

TABLE 1 A list of multibody interaction energy parameter sets used in this study

Multibody Interaction Energy Parameter Set	Energy Cost for Each Additional Chol-Chol Contact							Eq. 5 Coefficients						
								c_0	c_1	c_2	c_3	c_4	c_5	c_6
MIEP I	0	1	1	1	1	1	1	0	1	2	3	4	5	6
MIEP II	0	1	8	3	3	3	3	0	1	9	12	15	18	21
MIEP III	0	1	1	10	3	3	3	0	1	2	12	15	18	21
MIEP IV	0	1	2	3	4	5	6	0	1	3	6	10	15	21

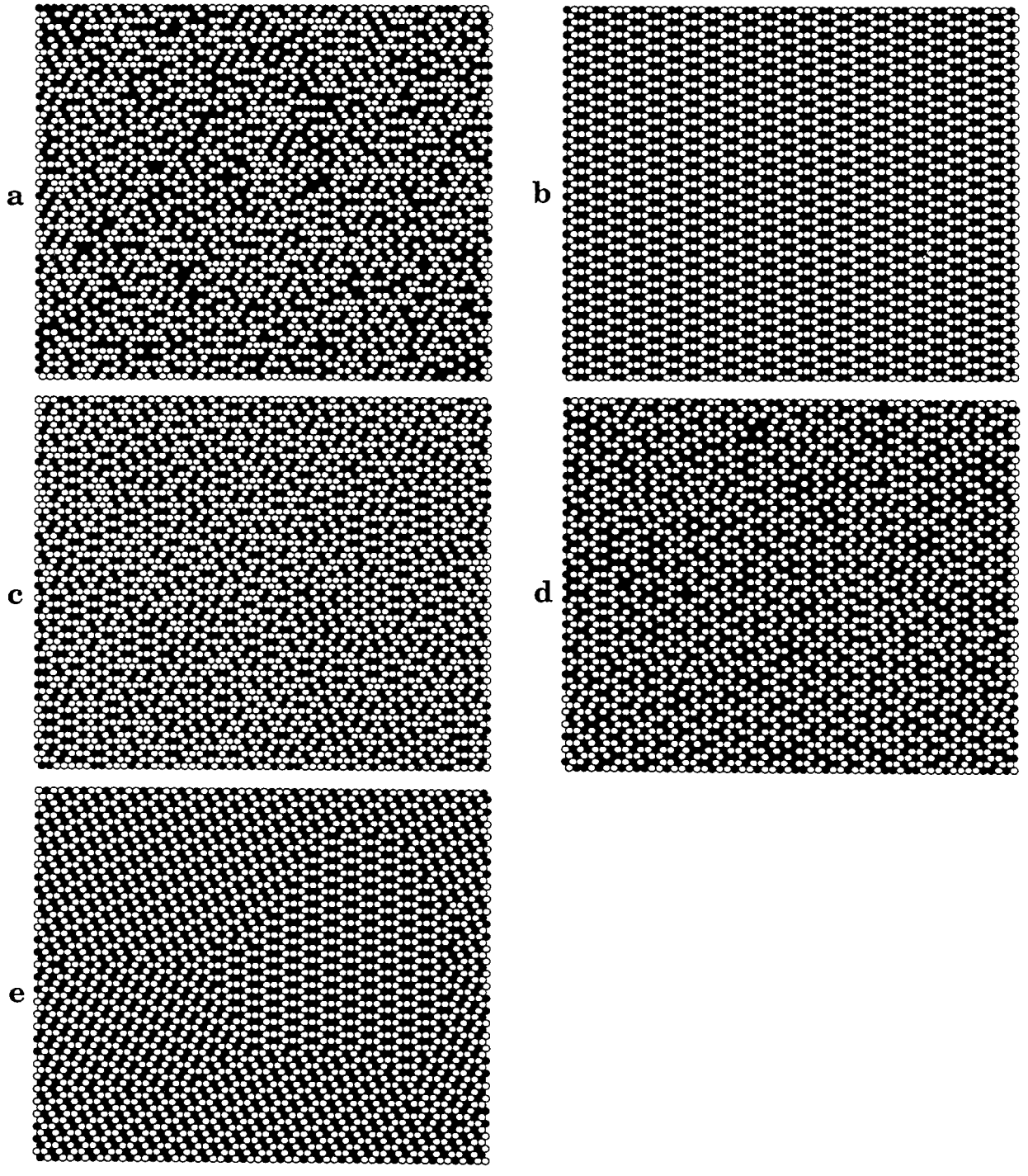

FIGURE 5 Snapshots of phospholipid and cholesterol lateral distributions simulated using MIEP II. (*a*) $\chi_{chol} = 0.57$ and $\Delta E_c = 0.2$ kT; (*b*) $\chi_{chol} = 0.57$ and $\Delta E_c = 0.5$ kT. Cholesterols form an aligned dimer pattern: each cholesterol has one other cholesterol as its nearest neighbor; (*c*) $\chi_{chol} = 0.51$ and $\Delta E_c = 0.5$ kT; (*d*) $\chi_{chol} = 0.62$ and $\Delta E_c = 0.5$ kT; (*e*) a metastable multidomain regular distribution at $\chi_{chol} = 0.57$ and $\Delta E_c = 0.6$ kT. (●) Cholesterol; (○) acyl chain.

multidomain distribution by slowly cooling down the mixture from a high temperature.

In MIEP III, we continue the assignment of large, unfavorable interaction energy to yet higher-order cholesterol-cholesterol contacts. In MIEP III, the 4-cholesterol multibody interaction is assigned the largest interaction energy. Fig. 2 *c* shows excess Gibbs free energy versus χ_{chol} simulated with MIEP III, and with ΔE_c ranging from 0 to 1 kT. ΔG^E has a sharp change in slope at $\chi_{chol} = 0.67$. The value of 0.67 is also a global minimum of ΔG^E.

The excess chemical potential of the mixture components is shown in Fig. 4, *c* and *d.* With $\Delta E_c \geq 0.3$ kT, $\mu_{chol}^{bilayer}$ has

an abrupt increase at $\chi_{chol} = 0.67$. The excess chemical potential of the acyl chains is plotted in Fig. 4 *d.* It shows the decrease at $\chi_{chol} = 0.67$ expected from the Gibbs-Duhem equation.

Fig. 6 shows snapshots of acyl chain-cholesterol lateral distributions simulated with MIEP III. In Fig. 6 *a,* at $\chi_{chol} = 0.67$, with a low magnitude of ΔE_c (0.1 kT), the distribution looks almost random: a cholesterol molecule could have from zero to six cholesterol-cholesterol contacts. However, at the higher ΔE_c of 0.6 kT shown in Fig. 6 *b,* cholesterol molecules form a "maze" pattern: the majority of cholesterols are surrounded by four acyl chains and two cholesterols. The majority of acyl chains are surrounded by four cholesterols and two acyl chains. Figs. 6 *c* and 10 *d* are snapshots of lateral distributions simulated with $\Delta E_c = 0.6$ kT at $\chi_{chol} = 0.60$ and 0.72, respectively. As χ_{chol} increases, the maze pattern that gradually forms at lower χ_{chol}, and encompasses the whole lattice at $\chi_{chol} = 0.67$, is gradually destroyed when χ_{chol} becomes higher. This indicates that both the formation and the disappearance of a regular distribution pattern are continuous phase changes.

MIEP III is formulated so that the *first two* cholesterol-cholesterol contacts only cost 1 energy unit each, but the third one costs 10 units, much higher than the first two. The energy costs for the fourth, fifth, and sixth contacts are not critical to produce the maze pattern, so we chose 3 for them. The mixture responds to MIEP III with a distribution that minimizes the third cholesterol-cholesterol contact, as shown in Fig. 6 *b.* This regular distribution pattern is a little more complicated than the other two. At $\chi_{chol} = 0.67$, the cholesterol/acyl chain ratio is 1/1. As shown in Fig. 7 *a,* by forming alternating lines of cholesterols and acyl chains, all the cholesterols can have exactly two cholesterols as nearest neighbors, and no additional cholesterol-cholesterol contacts occur. However, there are three possible orientations of the pattern in Fig. 7 *a* in a hexagonal lattice. In addition, the pattern shown in Fig. 7 *b* has an energy identical to that of the pattern in Fig. 7 *a,* and it can also be arranged in three possible ways. Unlike the multidomain aligned dimer pattern shown in Fig. 5 *e,* the patterns in Fig. 7 can switch from one orientation to another with relatively low energy penalty. The maze pattern is the result of this sixfold degeneracy.

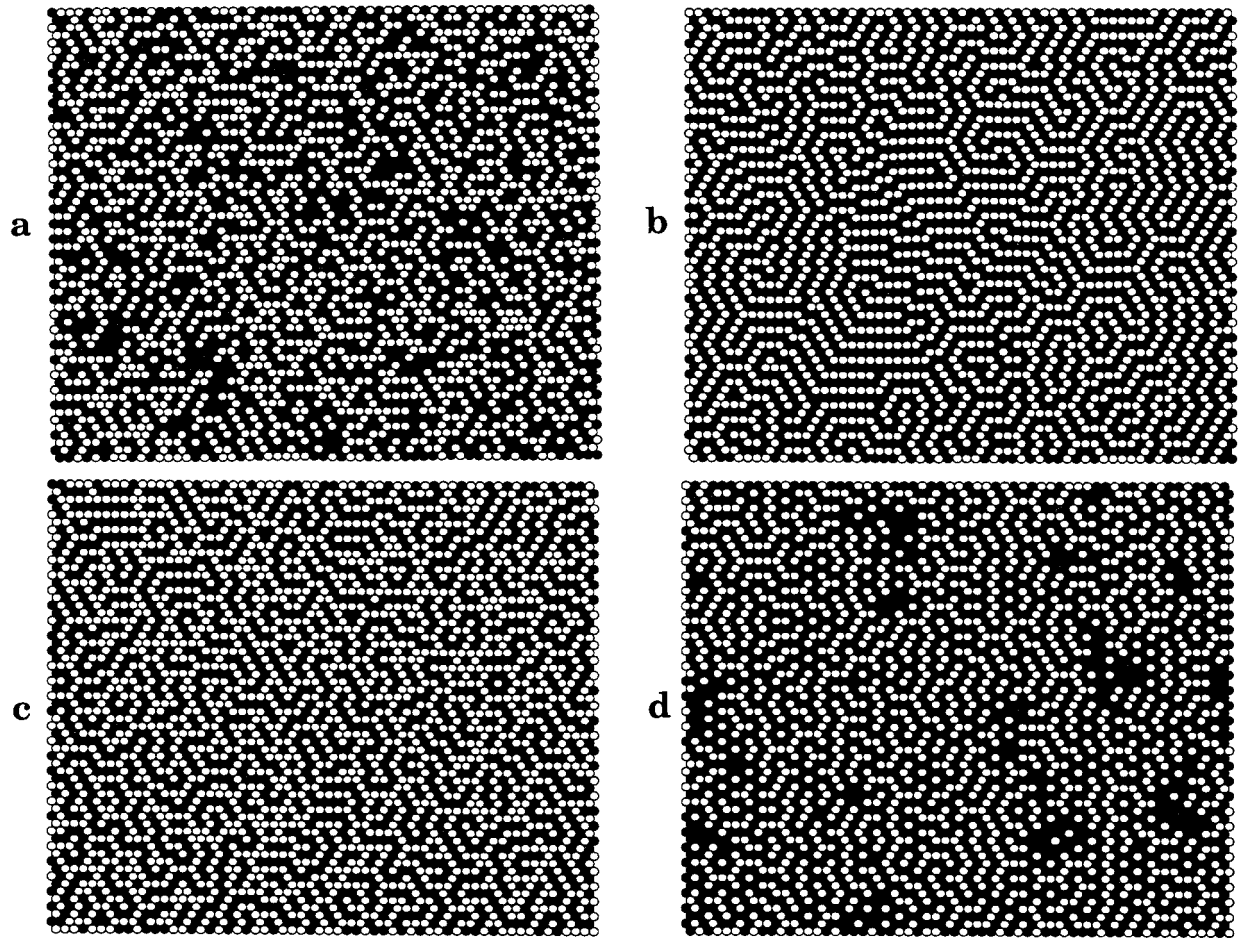

FIGURE 6 Snapshots of phospholipid and cholesterol lateral distributions simulated using MIEP III. (*a*) $\chi_{chol} = 0.67$ and $\Delta E_c = 0.1$ kT; (*b*) $\chi_{chol} = 0.67$ and $\Delta E_c = 0.6$ kT. Cholesterols form a maze pattern: each cholesterol has two other cholesterols as its nearest neighbors; (*c*) $\chi_{chol} = 0.60$ and $\Delta E_c = 0.6$ kT; (*d*) $\chi_{chol} = 0.72$ and $\Delta E_c = 0.6$ kT. (●) Cholesterol; (○) acyl chain.

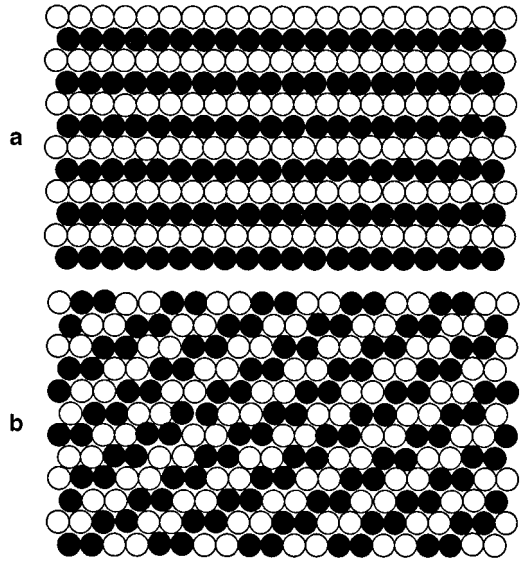

FIGURE 7 Two possible regular distribution patterns at $\chi_{chol} = 0.67$.

Consider a tiny amount of cholesterol added to the mixture to replace acyl chains and raising χ_{chol} by an infinitesimal amount above 0.67. The added cholesterol is forced into sites previously occupied by acyl chains having four cholesterol contacts. The newly added cholesterol now touches the four nearest-neighbor cholesterols already having three cholesterol-cholesterol contacts. The energy cost for such an operation would be very high. Therefore, the chemical potential of cholesterol sharply jumps at $\chi_{chol} = 0.67$.

In MIEP III, the third cholesterol-cholesterol contact is assigned to cost 10 energy units. In order to induce a sharp jump in chemical potential of cholesterol, ΔE_c needs to be $\geq$0.5 kT (Fig. 4 *c*). Thus, the actual energy cost for the third cholesterol-cholesterol contact should be $0.5 \times 10 = 5$ kT or higher.

MIEP IV in Table 1 is an interesting parameter set. The energy cost for each additional cholesterol-cholesterol contact was chosen to be 1 unit higher than the preceding one. Thus, c_i increases nonlinearly from 0 to 21. Fig. 2 *d* shows the excess Gibbs free energy versus χ_{chol} simulated using MIEP IV. Compared with MIEP I, II, and III, the slope change in ΔG^E at critical mole fractions is more subtle. Fig. 4 *e* shows the excess chemical potential of cholesterol versus χ_{chol}. This curve has three step increases for $\Delta E_c \geq 3$ kT: a steep jump at $\chi_{chol} = 0.5$, and more gradual rises at 0.57 and 0.67.

Fig. 8 shows a plot of ΔG^E and ΔH^E, together with $-T\Delta S^E$ for $\Delta E_c = 0.6$ kT, simulated with MIEP II. ΔG^E and ΔH^E are both at global minima at $\chi_{chol} = 0.57$. However, $-T\Delta S^E$ has a peak at $\chi_{chol} = 0.57$. This indicates that by forming the aligned dimer pattern at $\chi_{chol} = 0.57$, as in Fig. 5 *b,* the excess entropy ΔS^E is drastically reduced. The entropy part of the Gibbs free energy $-T\Delta S^E$ actually increases to a peak at $\chi_{chol} = 0.57$. Whenever a regular distribution is formed, regardless of the interaction type, the excess entropy, ΔS^E, reaches a minimum. Fig. 9 shows ΔS^E as a function of cholesterol mole fraction for a series of ΔE_m values, simulated using pairwise-additive interactions, or equivalently, using MIEP I. As ΔE_m becomes more negative, the crystal-like regular pattern at $\chi_{chol} = 0.50$ gradually forms (Fig. 3 *b*); by adopting fewer and fewer configurations in phase space, the entropy reaches a minimum at $\chi_{chol} = 0.50$. Once the pattern is completely formed at $\Delta E_m \leq -2$ kT, ΔS^E stops changing at $\chi_{chol} = 0.50$.

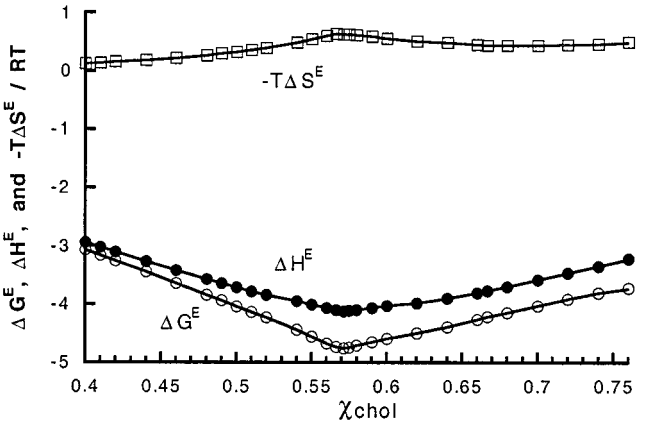

FIGURE 8 ΔG^E and ΔH^E, and $-T\Delta S^E$ as functions of cholesterol mole fraction, for $\Delta E_c = 0.6$ kT, simulated with MIEP II.

$-T\Delta S^E$ is always at a peak whenever a regular distribution occurs. In contrast, ΔH^E is always at a local (sometimes global) minimum; however, ΔG^E is not always at a minimum, but usually has a sudden change of slope at a regular distribution composition.

DISCUSSION

We have developed a model for cholesterol-phospholipid interactions in a bilayer having high cholesterol content. Our model focuses on the key finding that cholesterol precipitates from bilayer mixtures with PC at a cholesterol

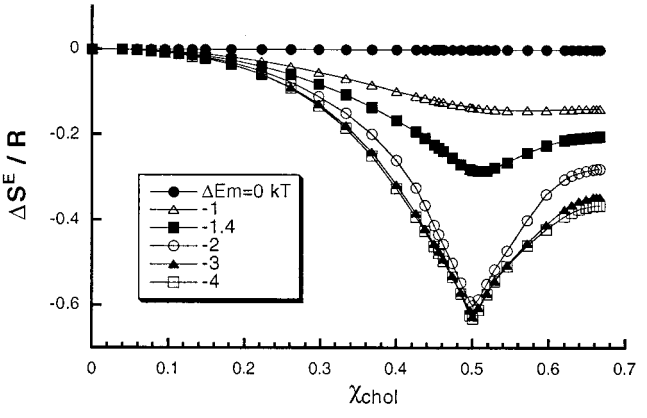

FIGURE 9 Excess entropy, ΔS^E, as a function of cholesterol mole fraction, at various values of ΔE_m, simulated using pairwise-additive interactions.

mole fraction of 0.66, and from bilayer mixtures of PE at 0.51. Our confidence in the precise numerical value of these mole fractions is based upon exhaustive experimentation described in recent papers (Buboltz and Feigenson, 1999; Huang et al., 1999).

We find that the most simple model for the microscopic interaction energies, in which cholesterol-cholesterol, cholesterol-phospholipid, and phospholipid-phospholipid energies are all pairwise additive, *can* explain the observed χ^*_{chol} value of 0.51 for 16:0,18:1-PE. This value of 0.51 appears naturally when the energy of unlike molecular contacts is sufficiently more favorable than the energies of like contacts (see Eq. 4). This is a common situation in mixtures, a form of nonideal mixing in which the mixing is better than random. However, if this pairwise additive description were adequate, then we would actually learn little about the physical origin of the interactions, since so many types of interactions fall into this category.

A key result from the thermodynamic analysis of our simulations is that the pairwise additive treatment *cannot* explain the observed χ^*_{chol} value of 0.66 for the four different PCs for which we have data. No choice of parameters in a pairwise additive model can yield a steep increase in $\mu^{bilayer}_{chol}$ (χ_{chol}) at $\chi_{chol} = 0.66$, as is shown in Fig. 4 *a*.

We could treat PE and the PCs separately, modeling the PC/cholesterol mixtures, but not the PE/cholesterol mixtures, with a *multibody* interaction energy treatment. However, we find that we gain insight by considering PE and PC to be described by the same general type of interaction parameter sets. In this general multibody interaction energy parameter (MIEP) model, we notice the number of cholesterol nearest-neighbors for each cholesterol in the lattice. We then assign the same energy to each cholesterol-cholesterol contact as in MIEP I, or we assign a gradual increase in energy as the number of multibody contacts increases as in MIEP IV, or else we assign a large jump in energy to particular contacts, e.g., to three-body contacts using MIEP II, or to four-body contacts using MIEP III.

Depending upon the choice of MIEP coefficients, that is, whether and how we assign energy jumps to particular cholesterol-cholesterol multibody contacts, computer simulations reveal different patterns for cholesterol-phospholipid lateral distributions:

1. There are three possible critical cholesterol mole fractions at which highly regular distributions of cholesterol can occur (see Note 3). They are $\chi_{chol} = 0.50$, 0.57, and 0.67, corresponding to cholesterol/phospholipid mole ratios of 1/1, 4/3, and 2/1, respectively. In these regular distributions, a cholesterol has exactly 0, or 1, or 2 other cholesterols as nearest-neighbors, if there are no defects in the distribution patterns.
2. When a regular distribution occurs, $\mu^{bilayer}_{chol}$ *always* jumps steeply at this critical mole fraction. If $\mu^{bilayer}_{chol}$ jumps high enough, it intersects $\mu^{crystal}_{chol}$. Thus, the MIEP model predicts that the measured χ^*_{chol} values are most likely to be in the vicinities of three possible critical cholesterol mole fractions. The enthalpy is always at a local (or global) minimum, indicating that a regular distribution is a minimum energy state. The entropy is also at a minimum, because the mixture adopts only a few particular configurations in phase space.
3. For the regular distribution to occur at $\chi_{chol} = 0.5$, the energy cost for every cholesterol-cholesterol contact must be higher than ~4 kT; for a regular distribution to occur at $\chi_{chol} = 0.57$, the energy cost for the additional, second cholesterol-cholesterol contact must be ~4 kT higher than that of the first one; and for the regular distribution to occur at $\chi_{chol} = 0.67$, the energy cost for the third cholesterol-cholesterol contact must be ~5 kT higher than that of the first two.

The umbrella model

In our cholesterol multibody interaction model, in order to have a steep jump in chemical potential at critical mole fractions, the energy cost for some higher-order cholesterol-cholesterol contacts must become much higher than that for lower-order contacts. Here, we propose a simple physical origin, which we term the "umbrella model," for the sudden increase in energy cost as cholesterols come into contact with each other in a bilayer.

Cholesterol is largely nonpolar. The lone hydroxyl represents <5% of the mass, and perhaps 1/4 of the surface that is exposed at the bilayer interface. Exposure to water of the nonpolar part of cholesterol would yield a very unfavorable contribution to the free energy (Privalov and Gill, 1988; Levy and Gallicchio, 1998). When cholesterols are incorporated into a phospholipid bilayer, phospholipid headgroups provide "cover" to shield the nonpolar part of cholesterol from exposure to water. This is illustrated schematically in Fig. 10 *a*. Phospholipid headgroups act like umbrellas. The space under the headgroups is shared by acyl chains and cholesterols.

As the cholesterol content in a bilayer increases, polar phospholipid headgroups reorient in order to provide more coverage per headgroup for the increasing fraction of cholesterol molecules, as drawn in Fig. 10 *b*. The headgroup umbrellas are "stretched" to provide more coverage area. Under the umbrella acyl chains and cholesterol molecules become tightly packed. No cholesterol is exposed to water at this point. Cholesterol hydroxyl groups also interact at the aqueous interface to provide partial coverage, but these hydroxyls cannot completely cover the nonpolar part of cholesterol without help from phospholipid headgroups.

For a given cholesterol molecule, an additional cholesterol nearest-neighbor comes at the cost of losing an acyl chain contact. If neighboring phospholipid headgroups are required to shield a given cholesterol from water, then we expect the energetic cost of each additional cholesterol-cholesterol contact to increase (see Note 4). In particular, if losing one more phospholipid contact would expose the cholesterol molecule to the aqueous phase, then the energy cost would jump sharply. As illustrated in Fig. 10 *c,* if the

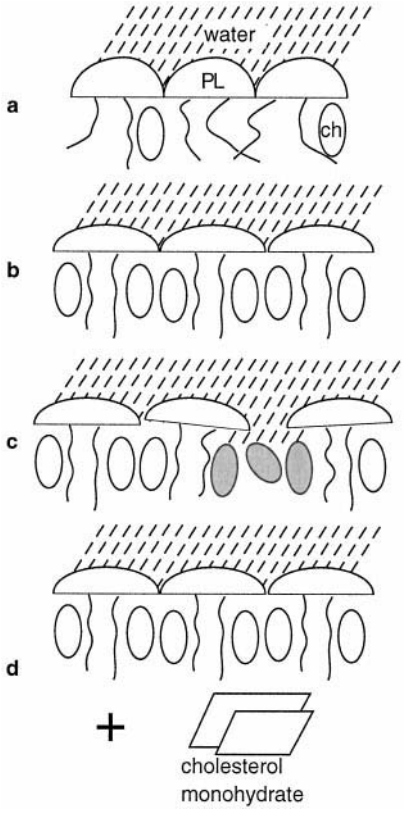

FIGURE 10 The physical origin of the maximum solubility of cholesterol in a bilayer, illustrated by the "umbrella model." Cholesterol molecules are represented as ovals. (*a*) In a lipid bilayer, the polar phospholipid headgroups act like umbrellas, shielding the nonpolar part of cholesterol molecules from water; (*b*) as the concentration of cholesterol increases, phospholipid headgroups are stretched to provide coverage for the increasing number of cholesterols; (*c*) the phospholipid headgroups are stretched to their limit and can no longer provide shielding for all cholesterol molecules. Some cholesterol molecules (*shaded ovals*) are exposed to water, causing a steep jump in chemical potential of cholesterol. (*d*) To lower the free energy, excess cholesterol molecules precipitate and form a second phase: cholesterol monohydrate crystals. The bilayer phase now contains the maximum number of cholesterols that the phospholipid headgroups can cover.

phospholipid headgroups are stretched to their limits, they can no longer provide shielding for additional cholesterols. Exposure of cholesterol to water is very unfavorable. This may well be the big increase in energy cost for acquiring an additional cholesterol-cholesterol contact (or equivalently, for losing an acyl chain contact) needed to produce the regular distribution of cholesterol and the steep jump of $\mu_{chol}^{bilayer}$ at critical mole fractions. To lower the overall free energy, instead of allowing the hydrophobic regions of bilayers to be exposed to water, excess cholesterol molecules precipitate, forming cholesterol monohydrate crystals, as shown in Fig. 10 *d.* Therefore, in our umbrella model, χ_{chol}^{*} has a physical meaning: χ_{chol}^{*} is a *cholesterol mole fraction at which the capability of phospholipid headgroups to cover cholesterol molecules from water has reached its maximum. Any additional cholesterol in the bilayer would be exposed to water.*

The difference in χ_{chol}^{*} values of PE and PC may originate from the size of their headgroups (Wilkinson and Nagle, 1981). Here, we mean the "effective area" of the headgroup, including bound water. The smaller headgroup of PE would be less effective than that of PC in providing shielding, so PE/cholesterol mixtures would have a high energy cost even for the first cholesterol-cholesterol contact. According to our simulations, relatively high energy cost for the first cholesterol-cholesterol contact results in $\mu_{chol}^{bilayer}$ rising sharply at 0.50, and thus $\chi_{chol}^{*} = 0.50$. In contrast, the larger headgroup of PC might well accommodate the first *two* cholesterol-cholesterol contacts, but be overwhelmed by the third one. The energy cost profile could then be modeled by MIEP III, i.e., very high energy cost for the third cholesterol-cholesterol contact. This would result in $\chi_{chol}^{*} = 0.67$. So if the size of the phospholipid headgroup is the dominating factor, then the lack of acyl chain dependence of χ_{chol}^{*} for PCs is explained.

Would the energy cost associated with aqueous exposure of cholesterol, together with any phospholipid deformations, be in the range of 4–5 kT, as estimated from our computer simulations? There are no data available for cholesterol-containing mixtures, but studies of the hydrophobic interaction and lipid deformation in other cases suggest that 4–5 kT is within the expected range. For example, King and Marsh measured the critical micelle concentration of spin-labeled PCs by ESR spectroscopy. They estimated the free energy of transferring a PC monomer from an aqueous phase to a micelle to be -1.1 kT per CH_2 group (King and Marsh, 1987). Fattal and Ben-Shaul calculated the lipid deformation free energy caused by lipid-protein hydrophobic mismatch in a bilayer, using a molecular model. At a mismatch length of 3.5 Å, the deformation free energy can be as high as 2 kT per lipid (Fattal and Ben-Shaul, 1993).

We have found only one other case in the literature where multibody interactions were used for membrane simulations. Drouffe and co-workers attempted to simulate a self-assembled two-dimensional membrane from individual amphiphilic "particles" using molecular dynamics simulations (Drouffe et al., 1991). They found that a membrane would not be stable unless a multibody interaction, which assigns a large free energy cost for exposing the hydrocarbon chains to water, is included in the simulation. This finding supports the importance of a hydrophobic effect as an essential membrane interaction.

The umbrella model and the "condensing effect"

The umbrella model implies the physical origin for the long-known "cholesterol condensing effect" (the average molecular area in a cholesterol-phospholipid monolayer is less than the sum; or, the range of motion of phospholipid acyl chains in a bilayer is reduced by cholesterol (Leathes, 1925; Demel et al., 1967; Stockton and Smith, 1976; Vist and Davis, 1990). These effects are also related to the decrease of bilayer permeability with increasing cholesterol

content (Kinsky et al., 1967). In the umbrella model, acyl chains and cholesterols become more tightly packed as cholesterol content increases, because they share the limited space under phospholipid headgroups. The hydrophobic nature of cholesterol thus forces cholesterol and acyl chains together. The model also implies that while acyl chains are compressed, phospholipid headgroups expanded.

Thus we propose that the hydrophobic interaction could be the common driving force for cholesterol precipitation from the bilayer, as well as for the condensing effect/acyl chain ordering.

Regular distribution and multibody interaction

The regular distribution pattern shown in Fig. 3 *b* is identical to one of the so-called "superlattice" distribution patterns of pyrene-PC or cholesterol in phospholipid bilayers. The proposed superlattice patterns were initially based on observation of a series of "kinks" or "dips" in the ratio of excimer-to-monomer fluorescence at particular mole fractions of pyrene-PC in bilayers (Somerharju et al., 1985; Tang and Chong, 1992; Chong et al., 1994). The bulky pyrene moieties were thought to form hexagonal superlattices in order to maximize separation from each other. Later, fluorescence data on cholesterol/phospholipid mixtures indicated that cholesterol molecules might also form superlattices in lipid bilayers (Chong, 1994; Virtanen et al., 1995; Liu et al., 1997). Superlattice patterns at $\chi_{chol} = 0.118$, 0.154, 0.20, 0.25, 0.33, 0.40, and 0.5 were suggested based on geometrical symmetry arguments. A regular distribution at $\chi_{chol} = 0.67$ (Fig. 7 *a*) has been proposed, but does not fit the general form of the superlattice (Lundberg, 1982; Virtanen et al., 1995). Sugar et al. explored the origin of superlattice patterns by using Monte Carlo simulations, introducing a long-range pairwise-additive repulsive interaction (Sugar et al., 1994). They found that long-range pairwise-additive repulsion can generate a superlattice pattern at $\chi_{chol} = 0.5$, like the pattern in Fig. 3 *b,* but cannot produce any other large-scale superlattice patterns. However, the general form of microscopic interaction that could produce the superlattices has remained unclear. In contrast, we have shown that the superlattice pattern in Fig. 3 *b* can also be generated with a nearest-neighbor pairwise-additive interaction, *without a long-range force.*

Pairwise-additive interactions are commonly used to model microscopic interactions between phospholipid molecules (Jorgensen and Mouritsen, 1995; Sugar et al., 1994; Huang et al., 1993), phospholipid and sterols (Cruzeiro-Hansson et al., 1989), as well as phospholipid and proteins (Zhang et al., 1993). In contrast, multibody interactions are rarely used for modeling lipid bilayers. This study clearly demonstrates that pairwise-additive interactions are inadequate to model the observed maximum solubility of cholesterol in bilayers; a multibody interaction is indispensable. The multibody interaction introduced in Eq. 5 can generate a series of regular distributions at $\chi_{chol} \geq 0.5$. This new class of regular distributions is based on molecular contact, *not* on maximum molecular separation, as proposed for the bilayer superlattices. It is interesting to note that the focus of the studies of Sugar et al. was to obtain a regular distribution of bulky molecules, whereas ours was to obtain a steep jump in cholesterol chemical potential. By calculating the free energy, we show that these two seemingly unrelated phenomena are actually the two inseparable consequences of a class of multibody interactions.

The usefulness of the multibody interaction treatment is not limited to description of the cholesterol interaction in bilayers of very high cholesterol content. It is readily extended to the low cholesterol content regime by introducing a different multibody interaction, associated with the local environment of each acyl chain. We have successfully simulated many cholesterol superlattice patterns at $\chi_{chol} < 0.5$ (Huang and Feigenson, manuscript in preparation). We can now conclude that regular distributions are generally created by multibody interactions.

Acyl chain effects

The chemical potential of cholesterol in bilayers must have some contribution from the microscopic interaction of cholesterol with its acyl chain neighbors. Cruzeiro-Hansson et al. (1989) calculated a cholesterol/phospholipid phase diagram for the low χ_{chol} regime, in which different interaction energies were assigned between cholesterol and acyl chains for different acyl chain conformations. We looked for such effects by measuring χ^*_{chol} in long- and short-chain PCs. The (pure PC) di22:1-PC bilayer is nearly 40% thicker than the di12:0-PC bilayer (Caffrey and Feigenson, 1981), so we might expect some difference in the interactions with cholesterol. Instead, we find that χ^*_{chol} are essentially identical in these two PCs, as well as in 16:0,18:1-PC and di16:0-PC, so the cholesterol-acyl chain contribution to $\mu^{bilayer}_{chol}(\chi_{chol})$ must be considerably smaller than that from cholesterol-cholesterol near χ^*_{chol}.

Our Hamiltonian is built to explore the cholesterol-cholesterol interactions that dominate in causing cholesterol precipitation near χ^*_{chol}. There are many other types of interactions that are included in our Hamiltonian, which could become dominant under different conditions. For example, at lower χ_{chol}, where cholesterol-cholesterol contacts are almost absent, cholesterol-acyl chain interactions could have an important role. However, the low χ_{chol} regime is not the focus of this study.

Absence of cholesterol-phospholipid complexes

As seen above, there are indeed "special mole ratios" of cholesterol/phospholipid, e.g., at 1/1 or 4/3 or 2/1. Distinct structural and thermodynamic events take place, such as the appearance of a regular distribution and a chemical potential jump. However, these special mole ratios that we identify

have *no connection whatsoever* to any chemical equilibrium binding reaction, such as $2\text{Chol} + \text{PL} \rightleftharpoons \text{PL(Chol)}_2$ or $4\text{Chol} + 3\text{PL} \rightleftharpoons \text{PL}_3\text{(Chol)}_4$. To clarify this point, consider the aligned dimer pattern at $\chi_{\text{chol}} = 0.57$ shown in Fig. 5 *b*. Superficially, it might appear to be a cholesterol-to-acyl chain stoichiometric 2/3 complex. However, at the lower cholesterol composition shown in Fig. 5 *c,* many cholesterol dimers are already formed, but no particular cholesterol/phospholipid ratio is associated with each dimer! The dimer pattern at $\chi_{\text{chol}} = 0.57$ is simply a minimum energy pattern, in which all cholesterols avoid the costly second cholesterol-cholesterol contact: *there is no chemical association between phospholipid and cholesterol.* In fact, there is no chemical association energy term in our Hamiltonian, and yet dramatic events can happen at "special mole fractions." Therefore, it is incorrect to generalize all distinct distributions that occur at special mole fractions to be complex formation.

Testable predictions

Our MIEP model predicts that χ^*_{chol} is most likely to occur at certain discrete values, in the vicinities of either $\chi_{\text{chol}} = 0.500$, or 0.571, or 0.667. So far, we found that four PCs have χ^*_{chol} at 0.66, and one PE at 0.51. Of course, more equilibrium χ^*_{chol} data for other phospholipids would provide a valuable test of this model.

$\chi^*_{\text{chol}} = 0.57$ is a new critical mole fraction that naturally arises from our model. There is no known report of χ^*_{chol} at 0.57 so far, nor have its regular distribution patterns (Fig. 5*b*) been described previously. Yet, the cholesterol-cholesterol multibody interactions that would give rise to these patterns and to $\chi^*_{\text{chol}} = 0.57$ would seem to be accessible, given the great variety of phospholipid headgroups. In terms of the microscopic energy, the requirement is that the three-body interaction of cholesterols should have a jump in energy, compared with the two-body cholesterol-cholesterol interaction, i.e., MIEP II should apply. It would be interesting to find some phospholipids having $\chi^*_{\text{chol}} = 0.57$. Reasonable candidates would be phospholipids with headgroup size intermediate between that of PE and PC, such as mono or dimethyl-PE. Mixtures of PE and PC might show $\chi^*_{\text{chol}} = 0.57$, for example if PE and PC in a bilayer mixture distribute randomly around cholesterol-cholesterol dimers.

If cholesterols do distribute regularly in bilayers at χ^*_{chol}, as pictured in Figs. 3 *b* and 6 *b,* such organization of cholesterol and acyl chains might be detectable, for example by neutron diffraction.

In this study we have partially characterized a particular interaction that dominates all others in the special case of binary phospholipid-cholesterol mixtures at high χ_{chol}. Although the study is restricted in this way, the finding of highly unfavorable cholesterol-cholesterol interaction seems applicable to real plasma membranes.

NOTES

1. In this simulation, two acyl chains belonging to the same phospholipid are not physically linked. A new simulation procedure to implement such a link has been recently reported (Sugar et al., 1998). We will try to incorporate it in our future simulations. We anticipate that this new procedure might have some effect on the entropy contribution to the Gibbs free energy.

2. In Fig. 4 and all other figures, χ_{chol} represents the cholesterol mole fraction in the bilayer. It can be different from the overall cholesterol content. For example, if the chemical potential jumps high enough at $\chi_{\text{chol}} = 0.5$ and reaches the value of $\mu^{\text{crystal}}_{\text{chol}}$, any additional cholesterol would precipitate to form cholesterol monohydrate crystals; $\mu^{\text{bilayer}}_{\text{chol}}$ would stop at the value of $\mu^{\text{crystal}}_{\text{chol}}$, and the cholesterol mole fraction in the bilayer would remain constant, even as the overall cholesterol content exceeds 0.5.

3. There are other theoretical critical mole fractions, higher than 0.67, at which regular distributions can occur (each cholesterol having three or more cholesterol contacts). Since we have not yet found an experimental χ^*_{chol} value higher than 0.67, we do not discuss these here.

4. The hydrophobic interaction has an overall unfavorable contribution to the free energy (Privalov and Gill, 1988; Levy and Gallicchio, 1998). At room temperature it is energetically favorable, but entropically very unfavorable. Since our lattice model does not explicitly contain water molecules, this unfavorable free energy contribution is phenomenologically expressed as an unfavorable interaction energy.

The authors thank Jeffrey Buboltz for many helpful discussions.

This work was supported by National Science Foundation Grant MCB-9722818.

REFERENCES

Bach, D., N. Borochov, and E. Wachtel. 1998. Phase separation of cholesterol in dimyristoyl phosphatidylserine cholesterol mixtures. *Chem. Phys. Lipids.* 92:71–77.

Bloch, K. 1991. Cholesterol: evolution of structure and function. *In* Biochemistry of Lipids, Lipoproteins and Membranes. D. E. Vance and J. E. Vance, editors. Elsevier, Amsterdam. 363–381.

Buboltz, J. T., and G. W. Feigenson. 1999. A novel strategy for the preparation of liposomes: rapid solvent exchange. *Biochim. Biophys. Acta.* (in press).

Caffrey, M., and G. W. Feigenson. 1981. Fluorescence quenching in model membranes. 3. Relationship between calcium adenosinetriphosphatase enzyme activity and the affinity of the protein for phosphatidylcholines with different acyl chain characteristics. *Biochemistry.* 20:1949–1961.

Chialvo, A. A. 1990. Determination of excess Gibbs free energy from computer simulation by the single charging-integral approach I. Theory. *J. Chem. Phys.* 92:673–679.

Chong, P. L.-G. 1994. Evidence for regular distribution of sterols in liquid crystalline phosphatidylcholine bilayers. *Proc. Natl. Acad. Sci. U.S.A.* 91:10069–10073.

Chong, P. L.-G., D. Tang, and I. P. Sugar. 1994. Exploration of physical principles underlying lipid regular distribution: effects of pressure, temperature, and radius of curvature on E/M dips in pyrene-labeled PC/DMPC binary mixtures. *Biophys. J.* 66:2029–2038.

Cruzeiro-Hansson, L., J. H. Ipsen, and O. G. Mouritsen. 1989. Intrinsic molecules in lipid membranes change the lipid-domain interfacial area: cholesterol at domain interfaces. *Biochim. Biophys. Acta.* 979:166–167.

Demel, R. A., L. L. M. van Deenen, and B. A. Pethica. 1967. Monolayer interactions of phospholipids and cholesterol. *Biochim. Biophys. Acta.* 135:11–19.

Drouffe, J. M., A. C. Maggs, and S. Leibler. 1991. Computer simulations of self-assembled membranes. *Science.* 254:1353–1356.

Fattal, D. R., and A. Ben-Shaul. 1993. A molecular model for lipid-protein interaction in membranes: the role of hydrophobic mismatch. *Biophys. J.* 65:1795–1809.

Finean, J. B. 1990. Interaction between cholesterol and phospholipid in hydrated bilayers. *Chem. Phys. Lipids.* 54:147–156.

Finegold, L. (editor). 1993. Cholesterol in Membrane Models. CRC Press, Boca Raton, FL.

Gershfeld, N. L. 1978. Equilibrium studies of lecithin-cholesterol interactions. I. stoichiometry of lecithin-cholesterol complexes in bulk systems. *Biophys. J.* 22:469–488.

Guggenheim, E. A. 1952. Mixtures. Clarendon Press, Oxford. 23.

Haile, J. M. 1986. On the use of computer simulation to determine the excess free energy in fluid mixtures. *Fluid Phase Equilibria.* 26: 103–127.

Horowitz, C., L. Krut, and L. Kaminsky. 1971. Cholesterol uptake by egg-yolk phosphatidylcholine. *Biochim. Biophys. Acta.* 239:329–336.

Huang, J., J. T. Buboltz, and G. W. Feigenson. 1999. Maximum solubility of cholesterol in phosphatidylcholine and phosphatidylethanolamine bilayers. *Biochim. Biophys. Acta.* (in press).

Huang, J., and G. W. Feigenson. 1993. Monte Carlo simulation of lipid mixtures: finding phase separation. *Biophys. J.* 65:1788–1794.

Huang, J., J. E. Swanson, A. R. G. Dibble, A. K. Hinderliter, and G. W. Feigenson. 1993. Nonideal mixing of phosphatidylserine and phosphatidylcholine in the fluid lamellar phase. *Biophys. J.* 64:413–425.

Jorgensen, K., and O. Mouritsen. 1995. Phase separation dynamics and lateral organization of two-component lipid membranes. *Biophys. J.* 69:942–954.

King, M. D., and D. Marsh. 1987. Head group and chain length dependence of phospholipid self-assembly studied by spin-label electron spin resonance. *Biochemistry.* 26:1224–1231.

Kinsky, S. C., S. A. Luse, D. Zopf, L. L. M. van Deenen, and J. Haxby. 1967. Interaction of filipin and derivatives with erythrocyte membranes and lipid dispersions: electron microscopic observations. *Biochim. Biophys. Acta.* 135:844–861.

Kirkwood, J. G. 1935. Statistical mechanics of fluid mixtures. *J. Chem. Phys.* 3:300–313.

Kirkwood, J. G. 1936. Statistical mechanics of liquid solutions. *Chem. Rev.* 19:275–307.

Leathes, J. B. 1925. Role of fats in vital phenomena. *Lancet.* 208:853–856.

Levy, R. M., and E. Gallicchio. 1998. Computer simulations with explicit solvent: recent progress in the thermodynamic decomposition of free energies and in modeling electrostatic effects. *Annu. Rev. Phys. Chem.* 49:531–567.

Liu, F., I. P. Sugar, and P. L.-G. Chong. 1997. Cholesterol and ergosterol superlattices in three-component liquid crystalline lipid bilayers as revealed by dehydroergosterol fluorescence. *Biophys. J.* 72:2243–2254.

Lundberg, B. 1982. A surface film study of the lateral packing of phosphatidylcholine and cholesterol. *Chem. Phys. Lipids.* 31:23–32.

Metropolis, N., A. W. Rosenbluth, M. N. Rosenbluth, and A. Teller. 1953. Equation of state calculations by fast computing machines. *J. Chem. Phys.* 21:1087–1092.

Nagle, J. F., R. Zhang, S. Tristram-Nagle, W. Sun, H. Petrache, and R. M. Suter. 1996. X-ray structure determination of fully hydrated $L\alpha$ phase dipalmitoylphosphatidylcholine bilayers. *Biophys. J.* 70:1419–1431.

Privalov, P. L., and S. J. Gill. 1988. Stability of protein structure and hydrophobic interaction. *Adv. Protein Chem.* 39:191–234.

Scott, H. L. 1991. Lipid-cholesterol interactions. *Biophys. J.* 59:445–455.

Somerharju, P., J. A. Virtanen, K. K. Eklund, P. Vainio, and P. K. Kinnunen. 1985. 1-palmitoyl-2-pyrenedecanoyl glycerophospholipids as membrane probes: evidence for regular distribution in liquid-crystalline phosphatidylcholine bilayers. *Biochemistry.* 24:2773–2781.

Stockton, B. W., and I. C. P. Smith. 1976. A deuterium NMR study of the condensing effect of cholesterol on egg phosphatidylcholine bilayer membranes. *Chem. Phys. Lipids.* 17:251–261.

Sugar, I. P., D. Tang, and P. L.-G. Chong. 1994. Monte Carlo simulation of lateral distribution of molecules in a two-component lipid membrane. Effect of long-range repulsive interactions. *J. Phys. Chem.* 98: 7201–7210.

Sugar, I. P., T. E. Thompson, K. K. Thompson, and R. L. Biltonen. 1998. Monte Carlo simulation of two-component bilayers: DMPC/DSPC mixtures. *Biophys. J.* 74:373*a.* (Abstr.).

Tang, D., and P. L.-G. Chong. 1992. E/M dips: evidence for lipids regularly distributed into hexagonal super-lattices in pyrene-PC/DMPC binary mixtures at specific concentrations. *Biophys. J.* 63:903–910.

Virtanen, J. A., M. Ruonala, M. Vauhkonen, and P. Somerharju. 1995. Lateral organization of liquid-crystalline cholesterol-dimyristoylphosphatidylcholine bilayers. Evidence for domains with hexagonal and centered rectangular cholesterol superlattices. *Biochemistry.* 34: 11568–11581.

Vist, M., and J. H. Davis. 1990. Phase equilibria of cholesterol/dipalmitoylphosphatidylcholine mixtures: ^{2}H nuclear magnetic resonance and differential scanning calorimetry. *Biochemistry.* 29:451–464.

Wilkinson, D. A., and J. F. Nagle. 1981. Dilatometry and calorimetry of saturated PE dispersions. *Biochemistry.* 20:187–192.

Zhang, Z., M. M. Sperotto, M. J. Zuckermann, and O. G. Mouritsen. 1993. A microscopic model for lipid/protein bilayers with critical mixing. *Biochim. Biophys. Acta.* 1147:154–160.